Investigation of the CECR2 bromodomain binding interactions with H2A.Z histone variants using a new AlphaScreen assay

A THESIS
SUBMITTED TO THE FACULTY OF THE GRADUATE SCHOOL
OF THE UNIVERSITY OF MINNESOTA
BY

Jacklyn Artymiuk

IN PARTIAL FULFILLMENT OF THE REQUIREMENTS
FOR THE DEGREE OF
MASTER OF SCIENCE

William C. K. Pomerantz, Ph.D.

August 2022

Acknowledgments

I would like to express my gratitude and sincere appreciation to my advisor, Professor William Pomerantz for his support, guidance, expertise, and patience throughout the research process over the past year. I would also like to acknowledge and thank all of the members of the Pomerantz lab for their unconditional willingness to provide training, assistance, and insight when needed. My heartfelt appreciation goes out to Professor Colin Campbell who patiently supported and believed in me throughout my entire degree program. His encouragement during some of my most difficult times allowed me to stay engaged and continuing forward. In this regard, I would also like to express my thanks to all of my instructors for their understanding, patience, and flexibility as well as to the University of Minnesota Department of Pharmacology for their continued support. Finally, I would like to extend my appreciation to Professors William Pomerantz, Colin Campbell, and Cheuk Leung for their willingness to participate as members of my thesis committee.

Abstract

A subset of epigenetic regulatory proteins modulate gene expression through structural domains called bromodomains which bind to N-ε-acetylations on histone protein lysine residues. Dysregulation of this process can have major impacts on gene expression and has been implicated in a number of cancers, inflammation, and neurological diseases. The histone variant H2A.Z isoforms are abundant in gene promoter regions and involved in transcriptional regulation. One bromodomain-containing protein that was recently shown to act at acetylated H2A.Z isoform sites is CECR2. Full characterization of CECR2's binding interactions with H2A.Z isoforms has yet to be determined but is crucial for understanding its role in transcriptional regulation and in disease. While prior studies used protein-observed ^{19}F NMR, the AlphaScreen assay is a more efficient characterization method. Therefore, the AlphaScreen assay's potential for characterizing these types of interactions was evaluated for characterizing the interactions of the CECR2 bromodomain and diacetylated H2A.Z peptide isoforms. Overall, this allows for both the better understanding of native CECR2 binding interactions and the optimization of a more efficient characterization method.

Table of Contents

List of Tables

List of Figures

Introduction

Epigenetics

At a time when the importance of genes and genetic inheritance had yet to be fully established, Conrad Waddington laid the foundation for the existence of additional mechanisms of inheritance coining the term epigenetics meaning "above genetics." Waddington defined epigenetics as, "the branch of biology which studies the causal interactions between genes and their products which bring the phenotype into being."[1,2] Epigenetic inheritance of a characteristic acquired in a population in response to an environmental stimulus was first demonstrated in 1956. Waddington knew that embryo fruit flies exhibited different thorax and wing structures in adulthood depending on their exposure to certain environmental factors. He therefore performed an experiment in which he selected for and bred fruit flies that displayed a bithorax phenotype upon environmental stimulation. After about 30 generations, he found that he could breed the flies and obtain robust inheritance of the bithorax phenotype in absence of the stimulus succeeding in showing that environmentally induced phenotypes can be inherited.[1,3] Epigenetics is therefore the study of heritable phenotype changes that do not involve alterations of the DNA sequence.[4] Waddington's findings revealed that the genetic code was no longer the only known basis for biological inheritance giving rise to epigenetic inheritance.

Epigenetic inheritance refers to the transmission of epigenetic memory which involves the mitotically and meiotically heritable changes made to a cell's gene expression profile induced by previous stimuli. There are multiple mechanisms that lead to epigenetic memory including DNA methylation, noncoding RNA-based mechanisms, incorporation of histone variants into nucleosomes, and histone protein modifications.[2, 5] Epigenetic memory can be a dynamic process allowing for adaptation in response to new environments before genetic adaption can evolve. However, it can also be stable and robust as seen in multi-cellular organisms in which cells having the same genome exhibit different phenotypes based on how the DNA sequence is expressed giving rise to distinct tissues with distinct functions through the process of cell

differentiation. These gene expression patterns are established during development and maintained throughout the life of the organism through epigenetic regulation.[6, 7, 8]

Epigenetic regulation is the process by which gene activity is regulated by the modification of chromatin structure. Epigenetic regulators are scaffolding proteins and enzymes that play a significant role in modulating gene expression through modifying the local state of chromatin and facilitating in the recruitment of essential members of the transcriptional machinery. Examples include three families of epigenetic proteins deemed writers, readers, and erasers referring to the enzymes that place epigenetic markers, proteins that recognize these marks, and enzymes that remove them, respectively. Epigenetic regulation plays a crucial role in many cellular processes including DNA replication, transcriptional regulation, cell cycle control, the DNA damage response, and reprogramming. The epigenetic regulation of these cellular processes has further downstream effects on biological processes such as embryogenesis, spermatogenesis, and memory formation.[9, 10] Therefore understanding the structure and dynamics of chromatin is crucial to understanding epigenetics and these vital processes.

Chromatin

Each human cell contains approximately 2 meters of DNA stretched out end-to-end. However, this DNA is housed in a ~10 μm diameter nucleus and therefore requires tight packaging.[14] The packaging of DNA serves multiple purposes including fitting the DNA into the nucleus, equal division of DNA during cell division, maintaining genome integrity, and maintenance of genome stability during cell division. This compaction of DNA structure is accomplished through the packaging of DNA into chromatin which is a complex of DNA and protein. In eukaryotic cells, chromatin consists of histone proteins and DNA condensed into repeating nucleosomal subunits each consisting of a core nucleosome, linker DNA, and often a linker histone protein.[15] The nucleosome constitutes the first level of DNA packaging and is the fundamental subunit of chromatin. Each nucleosome consists of about 147 base pairs (1.7 turns) of DNA wrapped lefthandedly around a set of eight proteins called histones, which form an

octamer containing two copies of each conserved histone: H2A, H2B, H3, and H4.[16] Often the nucleosome also consists of one H1 linker histone protein. H1 histones sit at the base of the nucleosome near the DNA entry and exit sites and bind to the linker region of the DNA.[5] Finally, nucleosomes also consist of linker DNA which are stretches of DNA, an average of 20 base pairs long, that connect the nucleosome particles (Figure 1).

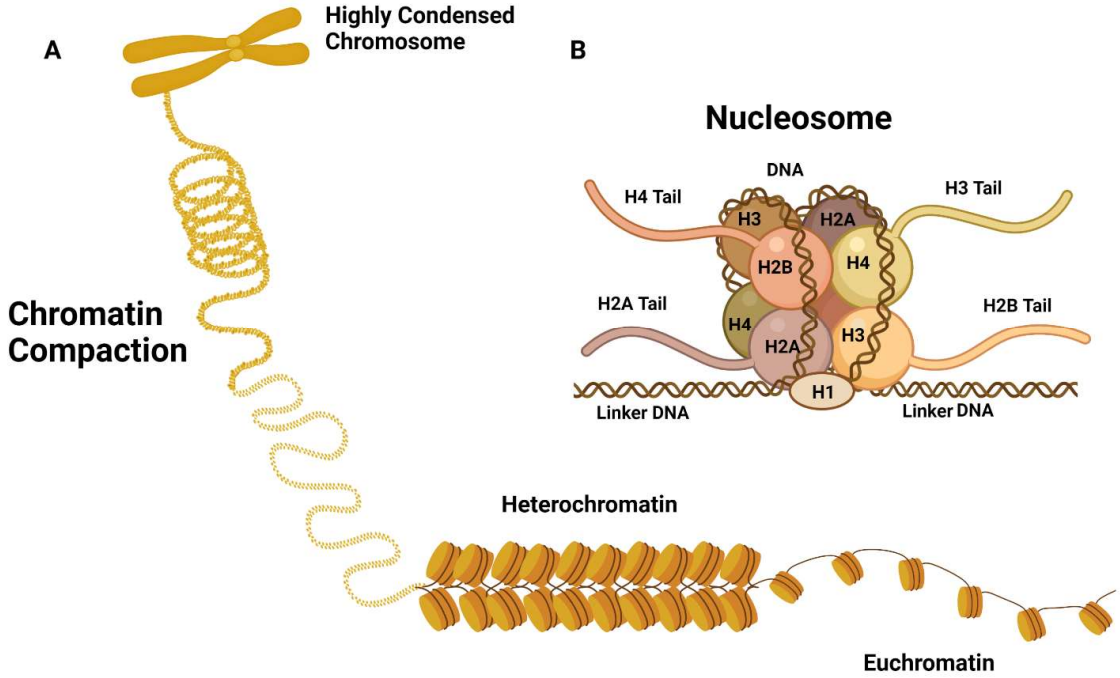

Figure 1: Nucleosome Structure and Chromatin Compaction. (A) Shown are the levels of chromatin compaction from the open structure of euchromatin to the tightly folded structure of heterochromatin. Chromosomes constitute the most highly condensed form of chromatin. **(B)** A single nucleosome is depicted consisting of the core octamer of histone proteins, linker DNA, and H1 linker histone protein. Four of the histone protein tails, which are the sights of histone epigenetic modifications, are also shown. Figure was created with Biorender.

This first level of DNA packaging into chromatin forms a "beads-on-a-string" structure when viewed under an electron microscope (Figure 2A).[17] This loose chromatin structure is called euchromatin and is a lightly packed form of chromatin that is often under active transcription. Overall, packaging the DNA into nucleosomes shortens the DNA fiber length sevenfold and protects it from damage while still allowing DNA polymerase full access to each base pair every cell cycle.[5] Despite this reduction in DNA fiber length, the chromatin is still too long to fit into

the nucleus. Therefore, it is coiled which involves the nucleosomes folding up into a tightly condensed, shorter, thicker structure termed the 30 nm fiber as it is approximately 30 nm in diameter (Figure 2B).[16] This more tightly condensed chromatin structure is called heterochromatin and is inactive for transcription.[17]

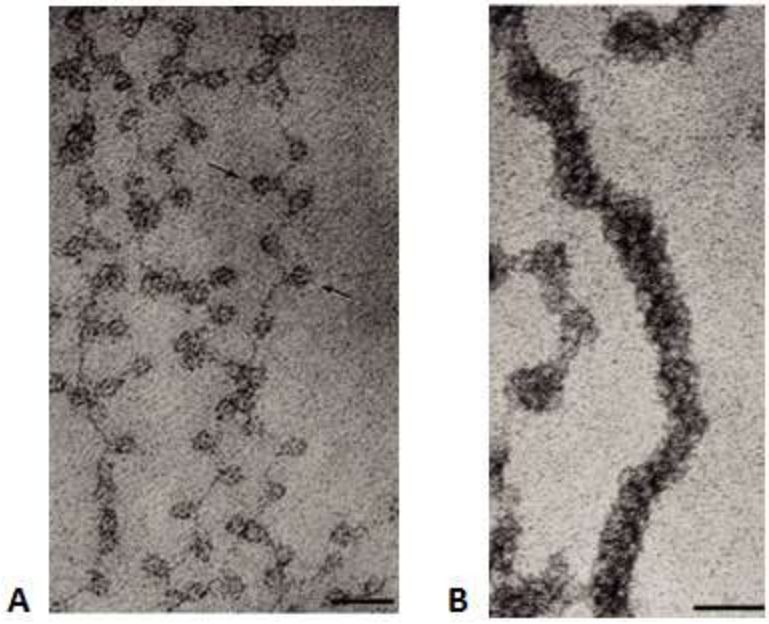

Figure 2: Chromatin Electron Micrographs. (A) Electron micrograph of euchromatin. The nucleosomes resemble beads on a string. Scale bar = 50 nm. **(B)** Electron micrograph of heterochromatin folded into a 30 nm diameter fiber. Scale bar = 50 nm. Both figures taken from Olins et al. 2003.[52]

While chromatin packaging is essential, it makes accessibility for epigenetic regulatory enzymes difficult. It is therefore vital for cells to have a way to transiently open the chromatin fibers permitting transcription, replication, and DNA repair. There are two main mechanisms that facilitate the accessibility of chromatin. These are the enzymatic modification of histone proteins and the incorporation of histone variants by chromatin remodeling complexes.[17] These processes are reversible, enabling modified or remodeled chromatin to be returned to its previous state.[17] Chromatin is therefore highly dynamic, and the chromatin of actively transcribed genes is in constant flux.[5]

Histone Proteins and their Variants H2A.Z I and II

The composition of nucleosomes can profoundly alter the chromatin structure and stability which is essential for the regulation of all DNA-based processes. As previously discussed, the nucleosome core particle is comprised of an octamer of two copies of each conserved histone: H2A, H2B, H3, and H4.[5, 18] The different positions of the core histones in the nucleosome subjected them to different evolutionary forces leading to the diversification of H2A and H3 but not H4 and H2B.[5] Therefore in humans H4 and H2B have only one isoform whereas H2A and H3 have several variants.[5] One of these variants is H2A.Z which is a highly conserved H2A variant with 60% identity to H2A. H2A and H2A.Z evolved nonoverlapping functions, and H2A.Z is essential in most organisms.[19] H2A.Z plays diverse roles in chromatin regulation.[5] Depending on the chromatin context and histone modifications, H2A.Z can act as a transcriptional activator or repressor giving it an important role in transcriptional regulation. H2A.Z-containing nucleosomes are enriched at the -1 and +1 nucleosomes surrounding the nucleosome depleted region of active promoters or transcriptionally poised genes.[19, 20] H2A.Z is incorporated into nucleosomes though a histone exchange at promotor sites. Its incorporation facilitates transcription by weakening DNA-histone interactions near the DNA entry and exit sites on the nucleosome and by mobilizing the +1 nucleosome. This enhances the DNA accessibility to RNA polymerase II which upon binding can initiate transcription. However, the local enrichment of H2A.Z when forming multiple adjoining H2A.Z nucleosomes promotes the formation of heterochromatin which inhibits the binding of the transcriptional machinery repressing transcription.[19] H2A.Z is also involved in a number of cellular processes including DNA replication and repair, cell cycle control, and stem cell differentiation and maintenance.[19, 20, 21, 22] This diversification of function most likely resulted from the evolution of two H2A.Z isoforms: H2A.Z I and H2A.Z II. H2A.Z is encoded by two different genes: H2AFZ and H2AFV leading to the production of three proteins, one produced from H2AFZ (H2A.Z.1) and two splice variants produced from H2AFV (H2A.Z.2 and H2A.Z.2.2) .[18, 20, 21] H2A.Z I and H2A.Z II differ by only

three amino acids with only one of these residues lying in the N-terminal tail region. However, they are nonredundant as the deletion of H2A.Z.I in mice is embryonic lethal.[18, 20, 22] Some independent functions for the H2A.Z variants have been found. A number of genes have been found to be regulated specifically by H2A.Z I and specifically by H2A.Z II.[20] They have also been found to regulate overlapping sets of genes, but in an opposite fashion meaning a number of the genes activated by H2A.Z I are repressed by H2A.Z II and vice versa.[20] H2A.Z I and H2A.Z II also regulate different sets of genes in different cells.[20] Facilitating the H2A.Z variants in transcriptional regulation are histone chemical modifications. One important modification in transcriptional activation is the acetylation of H2A.Z variant lysine residues.

Histone Acetylation

Vincent G. Allfrey was the first to suspect that histone proteins could be chemically modified and that these modifications played an important role in regulating transcription.[23] This work showed that modifying histone proteins with an acetyl group on the N-ε on lysine residues reduced their positive charge weakening their interaction with the negatively charged DNA and therefore leaving the underlying DNA exposed and more amenable to transcription.[23] Histone acetylation occurs primarily on the N-terminal tail of histone lysine residues and is catalyzed by histone acetyltransferases (HATs) and removed by histone deacetyltransferases (HDACs). Histone acetylation plays important roles in the regulation of a number of processes with the most widely investigated being transcriptional activation.[24] Histone acetylation affects transcription through two main mechanisms: by altering the interaction between DNA and histones as previously described and also through the recruitment of proteins requiring the binding of epigenetic reader proteins.[24] Acetylated lysine is recognized by the bromodomains (BRDs) of the epigenetic reader protein class of the bromodomain-containing proteins.

Bromodomains

Bromodomain-containing proteins are epigenetic reader proteins that selectively recognize and bind to acetylated lysine residues particularly on histone proteins. They play a

crucial role in transcriptional regulation and have a number of diverse functions including acetylating histones, remodeling chromatin, and recruiting other factors necessary for transcription. [24, 25, 26] There are 46 bromodomain-containing proteins with a total of 61 bromodomains in the human proteome. They are divided into eight major families according to sequence and structural homology (Figure 3).[26]

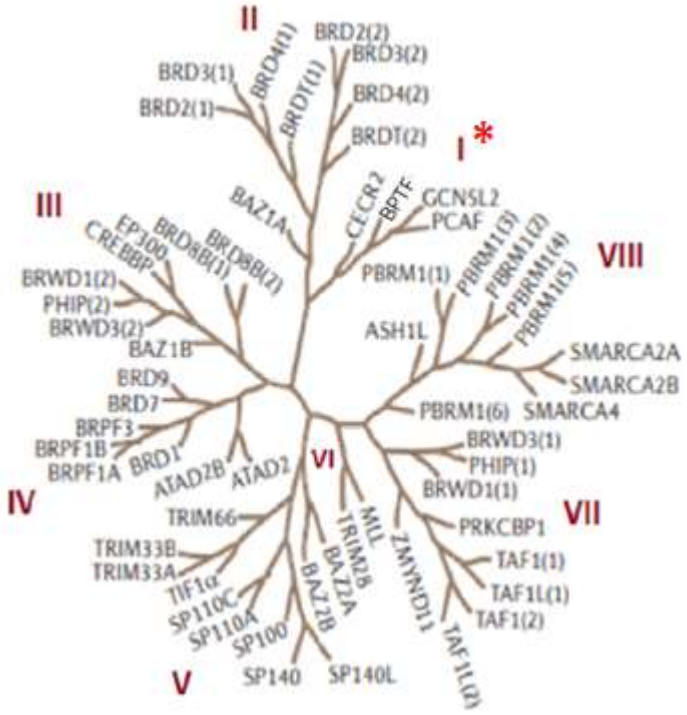

Figure 3: Human Bromodomain Phylogenetic Tree. Shown are the 61 human BRDs separated into eight families based on structural homology. Family I is starred as it is home to both the BPTF and CECR2 BRDs which are the two BRDs used in the research for this Master's thesis. Figure adapted from Filippakopoulos and Knapp. 2014.[53]

The bromodomain is well conserved despite the functional diversity of bromodomain-containing proteins. Structurally, BRDs consist of a left-handed bundle of four alpha helices (α_Z, α_A, α_B, and α_C) which are conserved across all BRDs. The hydrophobic acetylated lysine binding pocket is formed by a large loop between α_Z and α_A (the ZA loop) and a shorter loop between α_B and α_C (the BC loop). [24, 26] Two residues are responsible for acetylated lysine recognition and are conserved for the majority of BRD's. They include a tyrosine residue in the ZA loop and an asparagine residue in the BC loop. The tyrosine and asparagine residues form water-mediated and

direct hydrogen bonds with the lysine acetyl group, respectively (Figure 4).[26] This is the case for 48 of the 61 BRDs. In the other 13 BRDs the asparagine residue is replaced with either a tyrosine, threonine, or aspartic acid residue.[27] Certain bromodomains also display affinity for multiple acetyl groups on closely spaced lysine residues in the same binding pocket.[24, 26] Apart from the residues which are directly involved in acetyl-lysine binding, the overall sequence of BRDs is not highly conserved. Structurally aligning BRDs reveals considerable variability within their ZA and BC loops. These differences may account for the differences observed in BRD binding specificities.[24, 26]

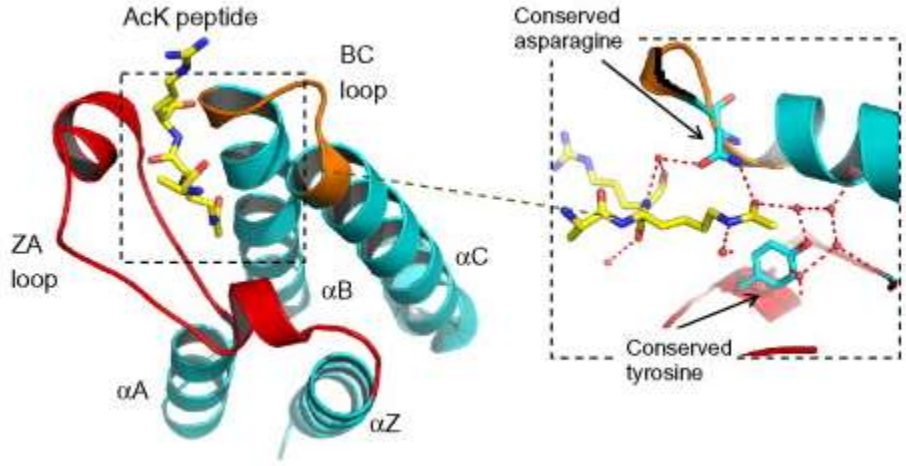

Figure 4: Bromodomain Structure and Binding. Shown are the key structures conserved across most BRDs. On the left are the four α-helices (Z, A, B, and C) and the structures forming the acetylated lysine binding pocket (ZA and BC loops). On the right are the conserved tyrosine and asparagine residues responsible for acetylated lysine recognition in the binding pocket. Depicted in yellow is an acetylated peptide engaged in a water-mediated hydrogen bond with tyrosine and a direct hydrogen bond with asparagine. Water molecules are depicted as spheres. Figure taken from Chung (2012).[57]

Bromodomains have recently proven their potential as druggable targets.[13] Within the past two decades seven epigenetic drugs have been approved by the FDA.[13] All of these drugs are inhibitors of either epigenetic writer or eraser proteins.[13] Although no drugs have yet been approved for targeting epigenetic readers, multiple inhibitors of the epigenetic reader domain, the bromodomain, have entered the clinic for their therapeutic potential in the treatment of cancer,

inflammation, and cardiovascular disease.[26] The family II bromodomain-containing proteins, referred to as the bromodomain and extra-terminal (BET) proteins, were among the first BRD-containing proteins whose biological roles as well as their roles in disease were extensively studied.[54] More non-BET bromodomain-containing proteins have also been implicated in disease making characterization of their native binding interactions important in establishing these roles.

The family I bromodomain-containing protein, bromodomain-and PHD finger-containing transcription factor (BPTF) has long been linked to transcriptional activity in a variety of cancers.[30] However, until recently little was known about its native binding interactions. BPTF was recently reported to selectively co-immunoprecipitate with H2A.Z-containing nucleosomes over H2A-containing nucleosomes in a chromatin immunoprecipitation (ChIP) experiment.[28] This prompted the characterization of the first direct interactions for acetylated H2A.Z with a bromodomain.[16, 29] In a subsequent study, all acetylated H2A.Z patterns with the BPTF bromodomain were characterized.[16]

H2A.Z histones contain five lysine residues on their N-terminal tails at positions 4, 7, 11, 13, and 15 and can be multi-acetylated.[16, 29] Mono-, di-, and tri- acetylation patterns on H2A.Z I and H2A.Z II peptide N-terminal tail interactions with BPTF were characterized by finding the binding affinities (K_d's) for each interaction by protein-observed ^{19}F (PrOF) NMR.[16, 29] It was found that diacetylation patterns enhanced the affinity of the peptide for BPTF over mono- and triacetylation.[16, 29] The K_d's of a panel of bromodomains with H2A.Z I and H2A.Z II peptides acetylated on lysines 7 and 13 (H2A.Z I AcK 7, 13 and H2A.Z II AcK 7, 13) were also found. This revealed that another family I bromodomain-containing protein, cat eye syndrome chromosome region, candidate 2 (CECR2), binds this acetylation pattern for isoform I with a K_d = 130 μM, which is the highest affinity reported in this study overall, and reported as non-saturating for isoform II suggesting potential isoform I selectivity.[16] This prompted the need to further characterize the CECR2 bromodomain interactions with the diacetylated H2A.Z I and II peptides.

It also prompted the investigation into CECR2's known biological role(s) and potential role(s) in disease.

CECR2's Biological Role and Role in Disease

It is well established that CECR2 is critical to the process of neurulation during embryonic development.[31] However, not much was known regarding CECR2's function in adult tissues until recently. It has been found to be involved in a number of processes. CECR2 is shown to be involved in both the female and male reproductive proesses.[32, 33] In female *Cecr2* mutant mice a number of defects are detected during early pregnancy suggesting a role for CECR2 in initiating and establishing pregnancy.[32] In males, CECR2 is involved in spermatogenesis with *Cecr2* mutants exhibiting reduced fertility.[33] CECR2 was also found to play a role in somatic cell reprogramming as an effector of Sall4 modulating the landscape of chromatin accessibility.[34] Finally, CECR2 has also been implicated in the DNA damage response by stimulating the formation of the phosphorylated histone variant γ-H2A.X and DNA double-stranded break repair.[35]

The role of CECR2 in disease has been unclear. CECR2's only known implication in cancer is in breast cancer metastasis reported in 2022.[36] Regardless, in the recent study the profiled transcriptomes of primary tumors and metastases revealed that CECR2 was the top up-regulated epigenetic regulator, and metastases showed that increased ratio of M2 macrophages correlated with higher CECR2 expression. The mechanism for CECR2's involvement in migration, invasion, and metastasis was found to occur through the NF-kB signaling pathway in which CECR2 binds to the acetylated lysine residues on the RelA/NF-kB complex leading to a pro-survival, proliferation, and pro-inflammatory response.[36] However, CECR2 is also a potential therapeutic target against metastatic diseases. NVS-CECR2-1 and GNE-886 are both inhibitors of the CECR2 bromodomain. When these inhibitors are used in mice implanted with 4T1 cells, CECR2 inhibition decreased the percent of total macrophages, decreased the percentage of M2 macrophages and increased M1 macrophages, and strongly inhibited the ability of the 4T1 cells to

metastasize.[36] Together these studies motivate the further study of native CECR2 protein interactions to gain a better understanding of CECR2's role in transcriptional regulation and in disease.

Thesis

To further establish CECR2 protein-protein interactions, the characterization of the CECR2 bromodomain binding interactions with diacetylated H2A.Z I and II peptides was one focus of this Master's thesis research (Figure 5).

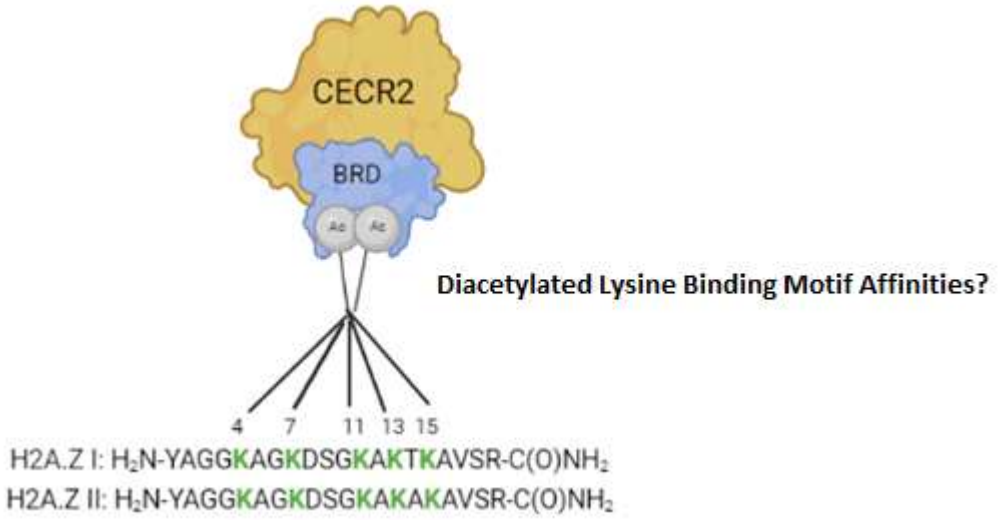

Figure 5: Thesis Focus 1. Characterization of diacetylated lysine binding motifs with H2A.Z isoforms and the CECR2 bromodomain. Figure created with Biorender and adapted from Perell et al. 2017.[29]

The other research focus involved the optimization of the AlphaScreen assay for the CECR2 bromodomain with H2A.Z I and II diacetylated peptides to evaluate the assay's potential for characterizing these types of interactions. The AlphaScreen assay is a high throughput assay that is faster and less material intensive than PrOF NMR and could greatly improve the characterization process.

Protein-observed ^{19}F (PrOF) NMR

Nuclear magnetic resonance (NMR) spectroscopy is a characterization technique used to observe local changes in chemical environment of NMR active nuclei by exposing them to an

external magnetic field. The response of these nuclei can provide detailed information regarding molecular structure, dynamic processes, and chemical reactions.[37] Only nuclei with nonzero values for spin can be used in NMR. Spin is the total angular momentum of a nucleus which gives rise to the nuclear magnetic moment. Common NMR-sensitive nuclei include ^{1}H, ^{13}C, ^{31}P, and ^{19}F.[43] When such sample nuclei are placed in a strong constant magnetic field (B_0) in an NMR instrument, their magnetic moments preferentially align with B_0, and their spin states split into two, with one aligned (lower energy) and one opposed (higher energy) to B_0.[40] When placed in a magnetic field charged particles precess about the field with a frequency of precession called the Larmour frequency.[40] If excited by a weak oscillating magnetic field with a frequency that matches the Larmour frequency (called a radio-frequency pulse), and applied orthogonally to B_0, nuclei in the lower energy spin state transition to the higher energy spin state absorbing radiation at the Larmour frequency.[40] As the nuclei spin states relax, radiation at the Larmour frequency is emitted and can be detected by sensitive radio receivers.[38, 39] The signal frequency, called the chemical shift (δ), is characteristic of the nucleus and its chemical environment.[38, 39, 40, 41] While there are many different types of NMR methods protein-observed ^{19}F (PrOF) NMR has become a valuable tool for the characterization of protein-ligand interactions.[51]

PrOF NMR is currently used as a ligand discovery tool through the study of protein-protein interactions and in fragment-based ligand discovery.[42, 40] However, it can also be used for characterizing protein interactions with their native ligands. Quantifying the dissociation constants (K_d's) of protein-ligand interactions using PrOF NMR first requires the expression of the fluorinated protein of interest through metabolic labeling of recombinant proteins in E-coli. The CECR2 bromodomain for example, contains a tryptophan (W) near the histone binding site W457. This tryptophan was fluorine-labelled as 5-fluorotryptophan (5FW) in past characterization studies using PrOF NMR.[16, 29] The K_d is then determined by performing a titration of the ligand and measuring the chemical shift response of the fluorinated protein resonance in the ^{19}F NMR spectra.[42] The changes in the chemical shift (Δδ) for each of the

different ligand concentrations can be plotted against the ligand concentration and used in a nonlinear least-square fitting to equation 1:

$$\Delta\delta_{obs} = \Delta\delta_{max}\frac{K_d + [L] + [P] - \sqrt{(K_d + [L] + [P])^2 - 4[PL]}}{2[PL]} \quad \textbf{(1)}$$

where $\Delta\delta_{max}$ is the maximum change in the fluorine chemical shift, [L] is the ligand concentration, [P] is the protein concentration, and [PL] is the bound complex concentration. The resulting does-response curve can be used to calculate the dissociation constant (K_d).[41] The relative ease and effectiveness of PrOF NMR experiments such as the latter owe a number of contributing key features to the ^{19}F nucleus.

As fluorine is rarely found in nature it provides a good chemical probe for a number of biological and chemical assays including NMR. This also typically results in simplified ^{19}F NMR spectra, and a broader array of solvents can be used as background signal suppression is no longer needed.[37, 38, 42] The ^{19}F nucleus also has a particularly high signal sensitivity and is hyperresponsive to subtle changes in its chemical environment with broad observable chemical shift ranges for fluorinated functional groups.[37]

One major limitation of PrOF NMR however, is that it can only be used for quantifying binding affinities with weak binding ligands that interact in the fast exchange regime.[41] Fast exchange is characterized by exchange between the free and bound states such that the total exchange rate is much greater than the chemical shift difference between the free and bound states' individual resonances.[51] As the total exchange rate is much greater than the chemical shift difference between the two states, the signals produced by each state average into one observable resonance on the NMR spectrum.[41] This allows for the observation of the change in the chemical shift for this one resonance throughout the titration.[41] Histone bromodomain interactions are relatively weak and tend to fall in the fast exchange regime making them good interactions to use with PrOF NMR.

Another major disadvantage of PrOF NMR is that it is relatively time consuming. Each data point, with two technical replicates, takes approximately 20 minutes to run on the NMR, and there are five datapoints per experiment. PrOF NMR experiments are also material intensive requiring nearly half the peptide yield from one synthesis and a relatively large amount of protein per experiment (typically 0.5 mL of 50 μM protein). An alternative assay of which is faster and less material intensive is called the AlphaScreen assay.[39]

AlphaScreen

AlphaScreen (Amplified Luminescent Proximity Homogenous Assay Screen) is a bead-based proximity assay[44, 48] utilizing two distinctly coated polystyrene beads, designated as donor and acceptor beads, that form pairs in the presence of an analyte.[49] Donor beads contain a phthalocyanine photosensitizer that when irradiated at 680 nm, excites ambient oxygen to a singlet state.[44, 49] Excitation of each donor bead generates approximately 60,000 oxygen singlets per second resulting in a highly amplified signal.[44] The singlet oxygen can travel up to 200 nm. Therefore, acceptor beads within this proximity receive singlet oxygen, and through its reaction with the dye contained in the acceptor beads, a chemiluminescent signal is produced through the emission of light from 520 nm to 620 nm.[44, 49]

The flexibility afforded by AlphaScreen in bead conjugation has enabled the development of numerous assays suitable for different biological applications including the activities of purified enzymes, the generation of second messengers, the detection of analytes involved cell signaling,[49] post-translational modifications to proteins and the characterization of different types of molecular interactions.[44] The latter of which includes protein-protein, protein-DNA, protein-RNA, protein-carbohydrate, protein-small molecule and receptor-ligand interactions.[47, 49] AlphaScreen is also used in high-throughput screening (HTS) to identify small molecule modulators for a variety of biological targets.[44]

The AlphaScreen assay here was optimized for the CECR2 bromodomain to characterize its interactions with diacetylated H2A.Z I and II peptides by performing competition assays. A

biotinylated peptide (H4 AcK 5, 8, 12, 16) probe which binds streptavidin donor beads and the His_9-tagged CECR2 bromodomain which binds the nickel chelate acceptor beads were used in these experiments. The protein-probe interaction brings the acceptor and donor beads into close enough proximity to generate a chemiluminescent signal upon excitation. Inhibitors of this protein-probe interaction reduce the proximity of donor and acceptor beads resulting in a signal decrease.[44] Therefore, a titration is performed with the diacetylated H2A.Z I and II peptides which bind competitively with the peptide probe to the CECR2 bromodomain producing greater signal inhibition with increasing concentration. The signal intensity is then plotted against the inhibitor concentration and the data fit to a sigmoidal 4-parameter logistic curve from which the IC_{50} values for the CECR2 bromodomain with the H2A.Z I and II peptides can be calculated (Figure 6).

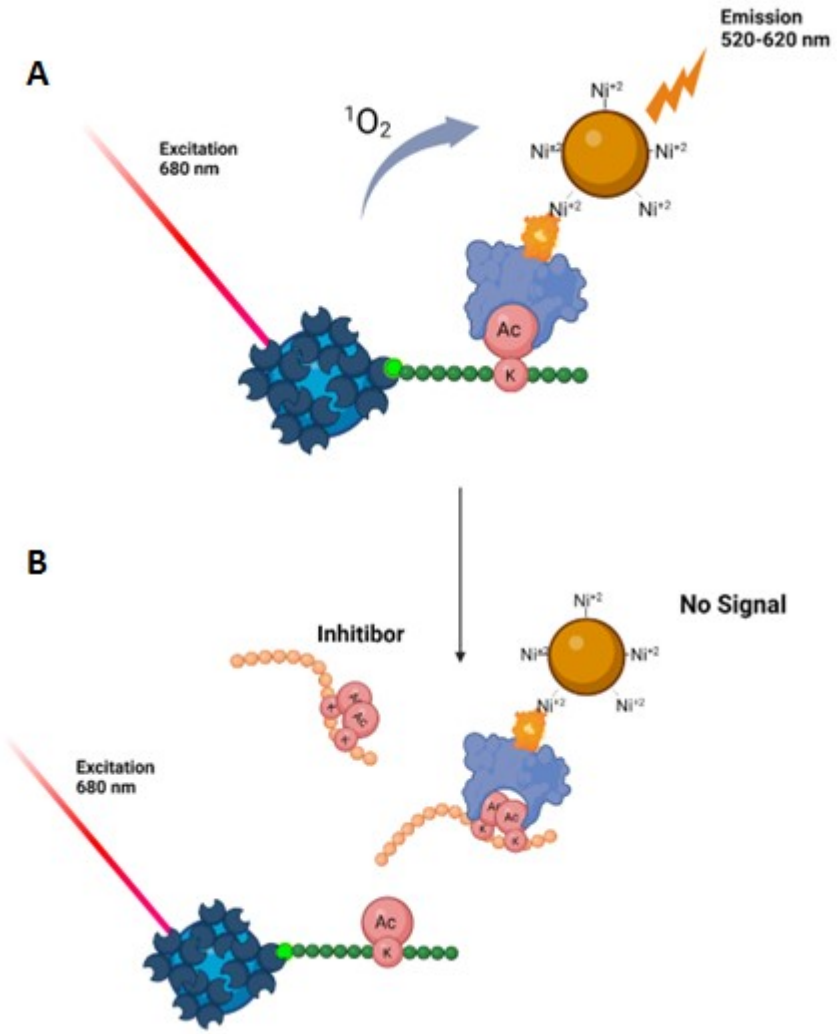

Figure 6: AlphaScreen Competitive Binding Inhibition Assay. (A) The bromodomain is allowed to interact with the acetylated lysine on the biotinylated peptide probe allowing for signal emission. **(B)** When an inhibitor is introduced, it competes with the probe for bromodomain binding decreasing the emitted signal intensity.
Figure created with Biorender.

A useful aspect of AlphaScreen is that it is highly sensitive allowing for the detection of low affinity interactions using only nanomolar reagent concentrations, minimizing the amount of each reagent needed.[47] The AlphaScreen competition binding assay therefore uses low levels of protein and probe in comparison to the dissociation constant for the protein-probe interaction (K_D). When applied to the Cheng-Prusoff equation (Equation 2):

$$K_d = \frac{IC_{50}}{1 + [P]/ K_D}$$

(2)

the low levels of probe [P] used are so much lower than K_D that the denominator is approximately one, allowing for the approximation of K_d from the IC_{50}.[50]

The AlphaScreen assay must be optimized for each new protein-protein interaction (PPI) to the specific system.[44] A number of factors must be considered including the optimization of the assay component concentrations using a cross-titration.[44] When the PPI components are titrated, both donor and acceptor beads become progressively saturated by their target molecules, and the signal increases with increasing protein concentration.[47] At the "hook" point, [47] either the donor or the acceptor component is saturated with the target molecule and a maximum signal is detected. Above the hook point, there is an excess of target molecules for the donor or the acceptor beads, which then inhibit their association and causes a progressive signal decrease.[47] When the affinity of the PPI is higher than the concentrations used in the assay, the hook effect can be masked, resulting in what looks like a traditional saturation curve rather than hooking. In this case, two competing equilibria are occurring: the signal is decreasing because of the hooking effect on the beads, but higher concentrations of protein drive the equilibrium toward more of the protein-protein complex.[47] Regardless, it is necessary to choose a protein concentration below the hook point for the assay.[49]

There are a number of other assay components to be considered when optimizing an assay for new PPIs including buffering agents, concentrations and pH. Generally, excellent performance has been reported with a number of buffers at concentrations ranging from 10 mM to 100 mM[47] at pH's ranging from 2.5 to 9. AlphaScreen assays can also tolerate a number of ions up to 300 mM in concentratons.[47] Many assays also require the use of detergents to prevent aggregation, ensure solubility and stability of components and to reduce non-specific binding.

AlphaScreen assays can tolerate the presence of a wide variety of detergents.[47] Proteins are commonly added to reduce the assay background noise including bovine serum albumin which can be tolerated up to 0.5% in solution.[47] Finally, the chemistry is designed to provide best results when the assay is performed at room temperature with an 8% variation in signal per °C deviation in room temperature observed.[49] As the CECR2 bromodomain interactions with the diacetylated H2A.Z I and II peptides have not yet been characterized using AlphaScreen, this type of assay optimization was required. However, first these specifically modified diacetylated peptides needed to be synthesized.

Results/Discussion

Peptide Synthesis

All peptides were synthesized via solid phase peptide synthesis using microwave irradiation and purified via reverse phase high performance liquid chromatography (Table 1). The peptide identities were verified using matrix-assisted laser desorption ionization (MALDI) mass spectrometry (see Table 8 in the Materials and Methods section below). The diacetylated H2A.Z I peptides were synthesized and used with the BPTF and CECR2 bromodomains in AlphaScreen competition experiments. Three additional peptides were also synthesized and used as negative controls in some of the AlphaScreen experiments. These were the unacetylated H2A.Z I peptide, the monoacetylated H2A.Z I AcK 13 peptide, and the H2A.Z II AcK 7, 13 peptide.

Table 1: Synthesized Peptides and their Sequences

Peptide	Sequence
H2A.Z I unAc	H_2N-YAGGKAGKDSGKAKTKAVSR-C(O)NH_2 *
H2A.Z I AcK 13	
H2A.Z I AcK 4, 7	
H2A.Z I AcK 4,11	
H2A.Z I AcK 4, 13	
H2A.Z I AcK 4, 15	
H2A.Z I AcK 7, 11	
H2A.Z I AcK 7, 13	
H2A.Z I AcK 7, 15	
H2A.Z I AcK 11, 13	
H2A.Z I AcK 11, 15	
H2A.Z II AcK 7, 13	H_2N-YAGGKAGKacDSGKAKacAKAVSR-C(O)NH_2

*Each acetylated H2A.Z I peptide is acetylated on the lysine residue (s) corresponding to the AcK numbers listed in the table.

AlphaScreen Competition Experiments with BPTF

While AlphaScreen competition experiments have been conducted with high affinity small molecules against related bromodomains to CECR2, very few experiments have been conducted with peptides and bromodomains in general and none with the CECR2 bromodomain. Following the synthesis and isolation of all H2A.Z peptides, AlphaScreen competition

experiments were performed. Prior to experiments with the CECR2 bromodomain, the BPTF bromodomain was first evaluated in order to gauge the accuracy of the assay by comparing the trend in IC_{50} results with literature PrOF NMR K_d values[16] for the H2A.Z peptides. Five diacetylated H2A.Z I peptides were selected for this analysis to assess the sensitivity and dynamic range of affinities that could be determined. Unexpectedly, while all peptides showed competitive inhibition, the obtained IC_{50} values were all significantly lower than the K_d values reported from PrOF NMR with only a small affinity difference between the peptides (using the stronger binding H4 AcK 5, 8, 12, 16 peptide with a K_d = 70 μM[50] and the weaker binding monoacetylated H2A.Z peptides with K_d's > 1000 μM[16] as references) (Table 2). The high standard deviations for experimental replicates also indicated high variability in the results and in the assay between experiments. However, the dose-response curves for each technical replicate retained a good fit (R^2= 0.97-0.99), and the IC_{50} values obtained for the control (small molecule BZ1 Figure 7A) for each experiment were in good agreement with the reported value of 0.067 μM.[55] A representative of the dose-response curves is shown in Figure 7B. Needless to say, it was difficult to draw any definitive conclusions regarding the accuracy of the assay from these results.

Table 2: BPTF AlphaScreen IC_{50}'s and Literature PrOF K_d's with Peptides

Peptide	AlphaScreen IC_{50} (μM)	Lit. PrOF K_d (μM)
H2A.Z I AcK 4, 11	200 ± 140[a]	780[d]
H2A.Z I AcK 4, 13	120	780[e]
H2A.Z I AcK 4, 15	110	630[e]
H2A.Z I AcK 7, 11	310[b]	1200[d]
H2A.Z I AcK 7, 13	220 ± 61[c]	520[e]

[a]Average of three experimental replicates. [b]Average of two experimental replicates. [c]Average of four experimental replicates. [d]Affinities previously reported by Perell et al.[29] [e]Affinities previously reported by Olsen et al.[16]

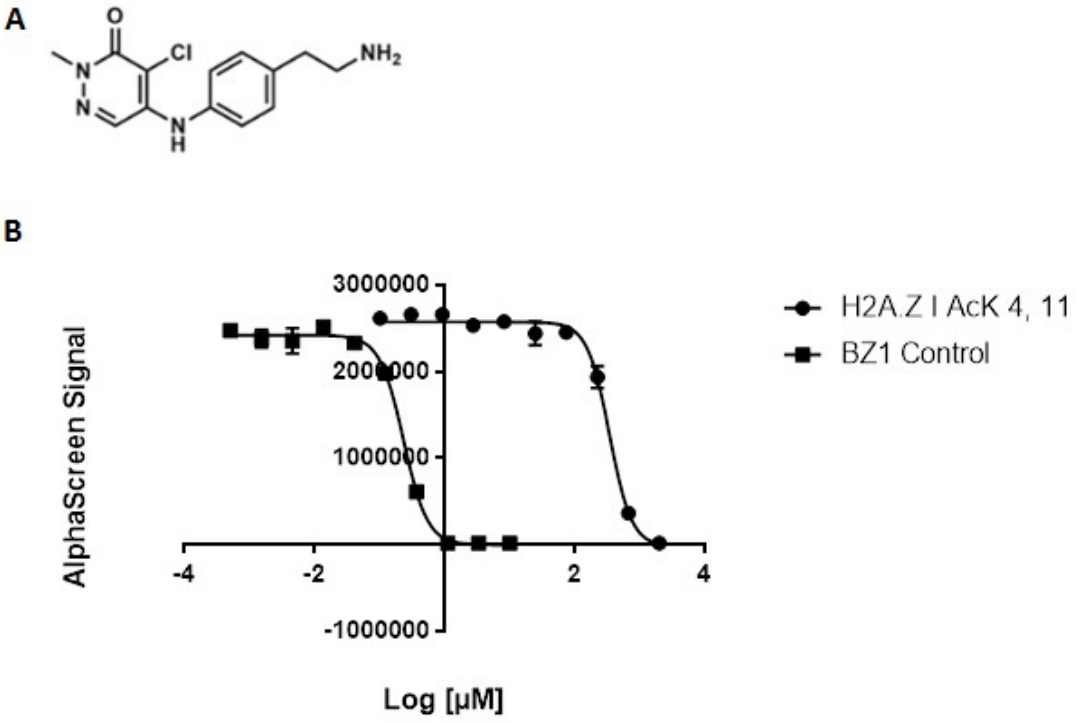

Figure 7: BZ1 Structure and Representative BPTF Dose-Response Curve. (A) Shown is the molecular structure for the small molecule bromodomain inhibitor BZ1 which is used as a positive control for all of the AlphaScreen experiments performed for this thesis. **(B)** Shown on the right is the dose-response curve obtained for BPTF and H2A.Z I AcK 4, 11 as a representative of the AlphaScreen assay dose-response curves obtained for BPTF and the diacetylated peptides. The curve on the left is the control BZ1. IC_{50} values were 340 μM for the peptide and 0.23 μM for the control (R^2=0.99 for both).

AlphaScreen Competition Experiments with CECR2

AlphaScreen competition experiments were also performed with CECR2 with seven of the diacetylated peptides for comparison to the BPTF bromodomain results. The IC_{50} results are shown in Table 3. PrOF NMR was also performed for CECR2 and the H2A.Z I AcK 7, 13 peptide. The K_d results as well as the literature K_d are also shown in Table 3. It is difficult to draw conclusions regarding the CECR2 IC_{50} values without being able to either validate the assay with BPTF PrOF NMR K_d data or to produce reproducible results. As with BPTF, experimental replicates had high standard deviations indicating high variability in the results and in the assay between experiments. All peptides did show competitive inhibition and the dose-response curves

for each technical replicate had a good fit. Also, the IC_{50} values obtained for the control (small molecule BZ1 Figure 7A) were reproducible for each experiment (no AlphaScreen IC_{50} data for CECR2 and BZ1 has previously been reported). A representative of the dose-response curves is shown in Figure 8, and the PrOF NMR binding isotherm for 5FW-CECR2 and the H2A.Z I AcK 7, 13 peptide is shown in Figure 9.

Table 3: CECR2 AlphaScreen IC_{50}'s and PrOF K_d's with Peptides

Peptide	AlphaScreen IC_{50} (μM)	PrOF K_d (μM)
H2A.Z I AcK 4, 11	130 ± 78[a]	
H2A.Z I AcK 4, 15	110	
H2A.Z I AcK 7, 11	120 ± 51[a]	
H2A.Z I AcK 7, 13	71 ± 41[a]	115, 130[b]
H2A.Z I AcK 7, 15	120 ± 43[a]	
H2A.Z I AcK 11, 13	240	
H2A.Z I AcK 11, 15	320	

[a]Average of three experimental replicates. [b]Affinity previously reported by Olsen et al.[16]

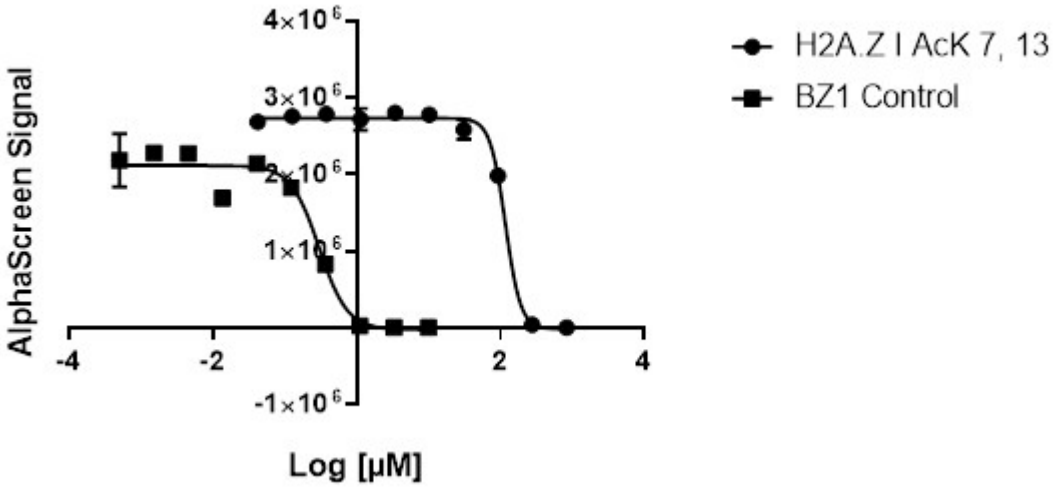

Figure 8: Representative CECR2 Dose-Response Curve. The curve on the right is the dose-response curve obtained for CECR2 and H2A.Z I AcK 7, 13 as a representative of the AlphaScreen assay dose-response curves obtained for CECR2 and the diacetylated peptides. The curve on the left is the control BZ1. IC_{50} values were 117 μM for the peptide and 0.30 μM for the control (R^2=0.99 and 0.97, respectively).

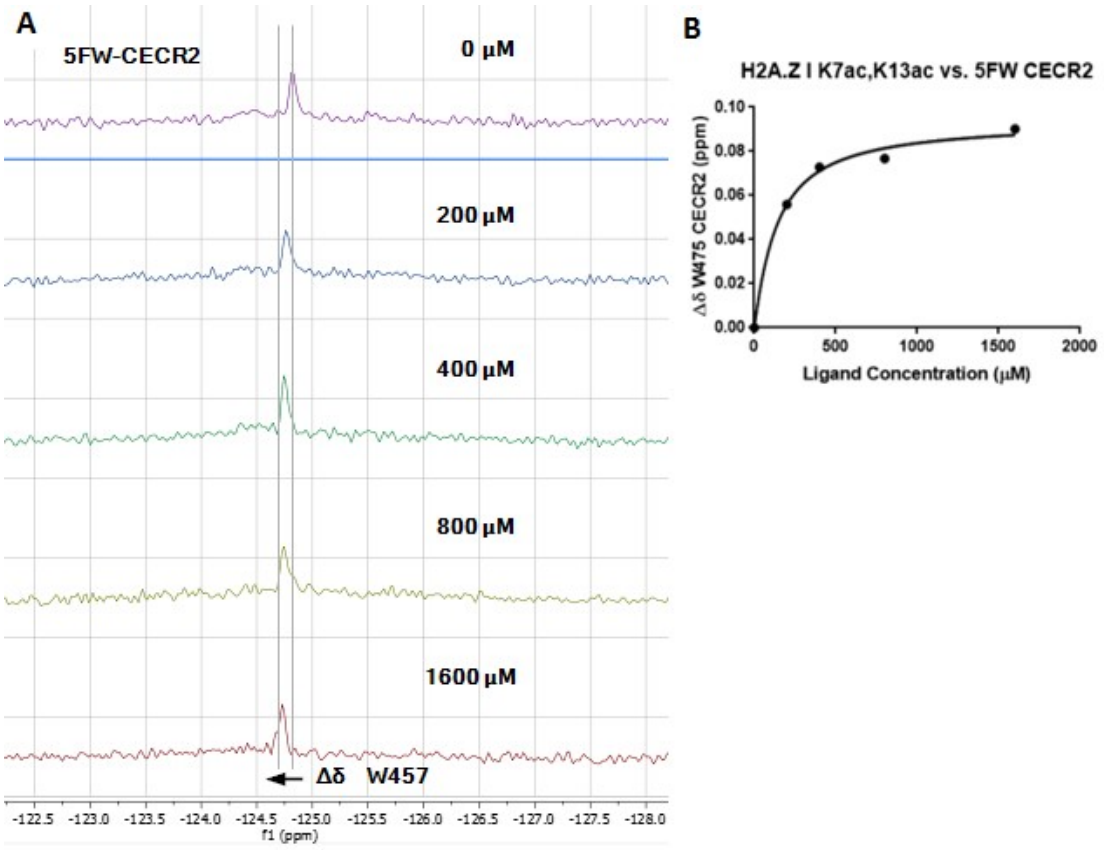

Figure 9: PrOF NMR Binding Experiment with H2A.Z I AcK 7, 13 and 5FW-CECR2. **(A)** Shown are stacked ^{19}F NMR spectra of 53 µM 5FW-CECR2 and increasing concentrations of the H2A.Z I AcK 7, 13 peptide showing the shift in the 5-fluorotryptophan resonance of W457 **(B)** Shown is the binding isotherm for the titration of 5FW-CECR2 with the H2A.Z I AcK 7, 13 peptide.

Negative Controls

As the IC_{50} values for BPTF were several-fold off from the PrOF NMR K_d values and could not be correctly rank ordered to the previously characterized peptides due to their narrow affinity range, AlphaScreen competition assays were performed using negative controls with both BPTF and CECR2 to determine the dynamic range for resolving different affinities. The negative controls were peptides reported as nonbinding, non-saturating, or weak binding (K_d > 1000 µM) to BPTF or CECR2. They included the unacetylated H2A.Z I peptide (nonbinding BPTF[16]), the monoacetylated H2A.Z I AcK 13 peptide (K_d = 1810 µM BPTF[16]), and the H2A.Z II AcK 7, 13 peptide (non-saturating CECR2[16]). Results from these experiments are shown in Table 4. Due to the variability in reported IC_{50} values for the negative controls with BPTF, the experimental

replicates were not averaged and each replicate is listed in Table 4. The IC_{50} values span from 240 μM to 110,000 μM for H2A.Z I unAc. As a nonbinder, the IC_{50} = 110,000 μM would be expected. However, this value was not replicated in any of the five additional experimental replicates. Instead, most of the results show low IC_{50} values for BPTF. Even the weak binder H2A.Z I AcK 13 produced IC_{50} values much lower than the expected K_d = 1810 μM with the exception of the IC_{50} = 40,000 μM which may be expected of a nonbinder but not the weak binding H2A.Z I AcK 13 peptide. Low IC_{50} values were also obtained for CECR2 although no experimental replicates were performed. These lower-than-expected IC_{50} values with non- and weaker binding peptides suggests a non-specific binding interaction or assay incompatibility. However, the highly variable results for BPTF made further conclusions difficult.

Table 4: IC_{50} Values for BPTF and CECR2 with Negative Controls

Peptide	AlphaScreen IC_{50} (μM)	Lit. PrOF K_d (μM)
BPTF		
H2A.Z I (unAc)	1300	NB[a]
	280	
	240	
	110000	
	660	
	770	
H2A.Z I AcK 13	40000	1810[b]
	31	
	320	
CECR2		
H2A.Z (II) AcK 7, 13	100[c]	NS[a]
H2A.Z I (unAc)	350	
H2A.Z I AcK 13	190	

[a]Affinity previously reported by Olsen et al.[16] [b]Affinity previously reported by Perell et al.[29] [c]Average of two experimental replicates.

pH Experiments

The unexpected higher affinity of both binding and nonbinding peptides, led to the investigation of an assay artifact that could be influencing binding behavior. The pH was therefore investigated first as the peptides were purified as trifluoroacetate salts, and residual trifluoroacetic acid was thought to affect the pH. It was then found that the highest concentration solution in the AlphaScreen serial dilutions for the peptides was acidic with an estimated pH of 5.0 (determined using pH tape). The stock peptides are diluted in AlphaScreen buffer to produce the AlphaScreen serial dilutions. The AlphaScreen buffer's pH is adjusted to 7.4. Therefore, the pH of these solutions should remain at 7.4. The highest concentration serial dilution for the nonpeptide control BZ1 was at a neutral pH as expected. Therefore, two experiments were performed to determine if pH has an effect on IC_{50} values. For the first experiment, AlphaScreen competition assays were performed using four different AlphaScreen buffers with the pH adjusted to 7.4, 6.8, 5.5 and 4.0 using BZ1 and CECR2. In this experiment, an IC_{50} of 0.17 μM was obtained for the buffer at pH=7.4, but no signal was obtained for the three lowest pH buffer solutions. Therefore, a second experiment was performed using a narrower pH range of 7.4, 7.2 and 7.0 for the AlphaScreen buffer solutions. In this case a decreasing trend in both IC_{50} and signal intensity with decreasing pH was observed as shown in Table 5 and Figure 10. The decrease in signal intensity indicates that there is a weaker interaction between the biotinylated peptide probe and the CECR2 bromodomain, and the decrease in IC_{50} indicates that it is easier for BZ1 to disrupt the probe-CECR2 complex.

Table 5: Varying pH with CECR2 and BZ1

Buffer pH	AlphaScreen IC_{50} (μM)	Max. Signal Intensity
7.4	0.17	1700000
7.2	0.097	600000
7.0	0.064	270000

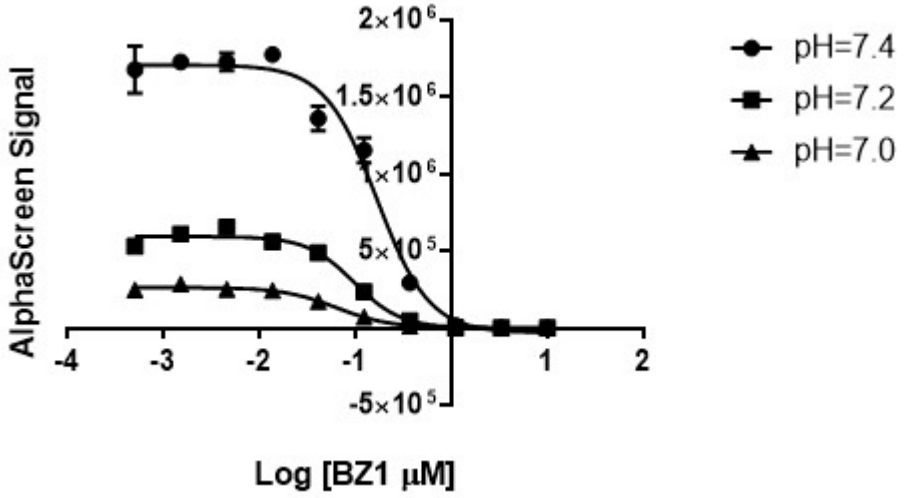

Figure 10: Varying pH with CECR2 and BZ1. Dose-response curves for CECR2 with BZ1 using three differently pH adjusted buffers (pH = 7.4, 7.2, and 7.0). The decrease in signal intensity with the decrease in pH is apparent. R^2 = 0.99, 0.98, and 0.99 for the pH = 7.4, 7.2, and 7.0 curves, respectively.

Buffer Capacity Experiments

Given the significant pH effect on the IC_{50} values, the buffering capacity of the AlphaScreen buffer was adjusted. Four solutions of differing buffer capacity were prepared (i.e., 25 mM, 50 mM, 100 mM, and 150 mM Na HEPES). For this experiment, it was expected that the IC_{50} values for the assays performed using the 100 mM and 150 mM buffers would increase relative to the IC_{50} values obtained for the assay performed with the standard 50 mM solution. This result was expected because the higher buffer capacities should better maintain the optimized pH of 7.4 and prevent the decrease observed in IC_{50} values with decreasing pH. To qualitatively assess the buffering capacity, the pH of each of the highest concentration serial dilution solutions was determined using pH tape. As expected, the solutions with the 25 mM and 50 mM buffers were acidic with a pH of about 5.0. Alternatively, the acidity of the solution with the 100 mM buffer was slightly reduced, and the solution with the 150 mM buffer was neutral. Raising the buffer capacity therefore did effectively maintain the pH. However, it should be noted that the AlphaScreen assay performance has only been tested using buffering agents including HEPES at concentrations between 10 mM – 100 mM.[47]

AlphaScreen competition assays were then performed using each buffer with BPTF and the H2A.Z I AcK 7, 13 peptide (chosen arbitrarily) with BZ1 as the control for each experiment. However, the expected increase in IC_{50} values for BPTF and the peptide using the 100 mM and 150 mM buffers was not observed (Table 6). No trend was observed for the buffer capacity and the IC_{50} values nor for the buffer capacity and maximum signal intensity. Dose-response curves are shown in Figure 11.

Table 6: Varying Buffer Capacities with BPTF

Buffer Conc. (mM)	AlphaScreen IC_{50} (µM)	Max. Signal Intensity
H2A.Z I AcK 7, 13		
25	290	2600000
50	170	2400000
100	270	2500000
150	140	2000000
BZ1 Control		
25	0.142	2500000
50	0.167	2300000
100	0.226	2500000
150	0.05	1700000

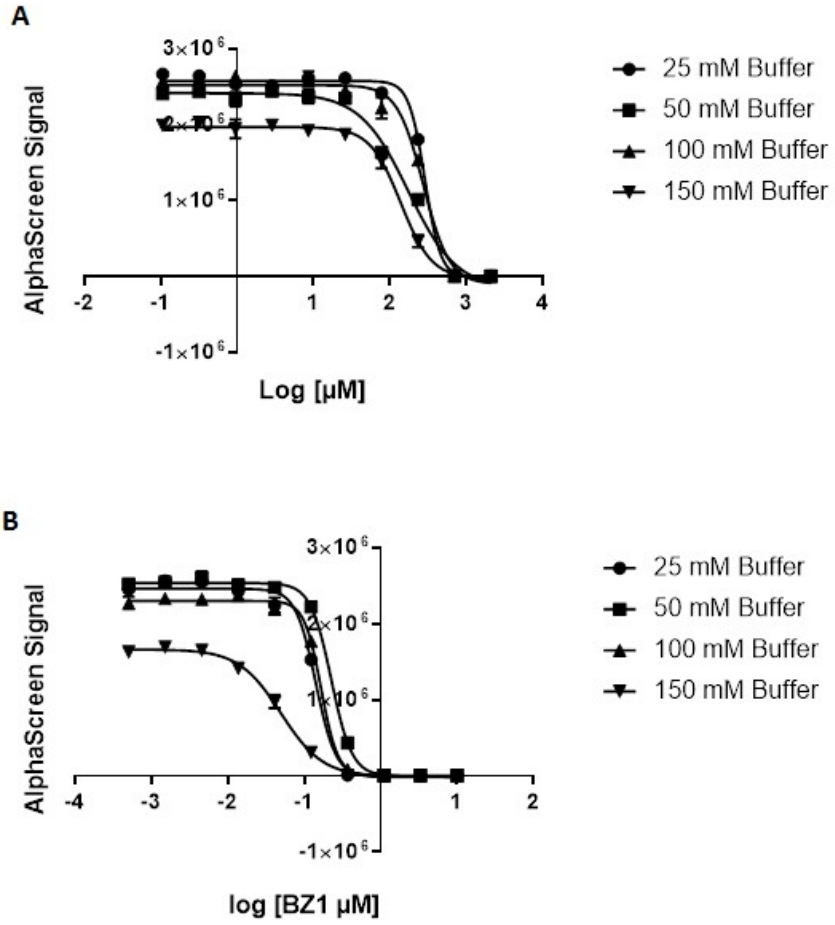

Figure 11: Varying Buffer Capacities with BPTF and H2A.Z I AcK 7, 13. (A) Shown are the overlain dose-response curves from the AlphaScreen assays for BPTF and H2A.Z I AcK 7, 13 performed using four different buffer strengths. **(B)** Shown are the dose-response curves for the control assays performed with each respective buffer strength using BZ1. (R^2 = 0.99 for all curves)

While the positive control binding affinities were unaffected by the buffer capacity, the negative controls were next evaluated. Since the 150 mM buffer could effectively buffer the acidic highest concentration serial dilution solutions to a neutral pH, the AlphaScreen assay was performed using the 150 mM buffer with negative controls for both BPTF and CECR2 (Table 7 and Figure 12). In this case, the H2A.Z I unAc peptide with BPTF showed non-binding behavior. However, the poor fit of the data, and the low signal intensity relative to the control was noted. In the context of CECR2, the IC_{50} value obtained for the negative control peptide H2A.Z I unAc was much lower than expected falling into the IC_{50} range expected for the diacetylated peptides. It

should also be noted that the control for this assay had half the signal intensity of that reached for the peptide.

Table 7: Negative Controls using 150 mM Buffer

Peptide	AlphaScreen IC50 (μM)
BPTF	
H2A.Z I (unAc)	1700000
CECR2	
H2A.Z I (unAc)	620

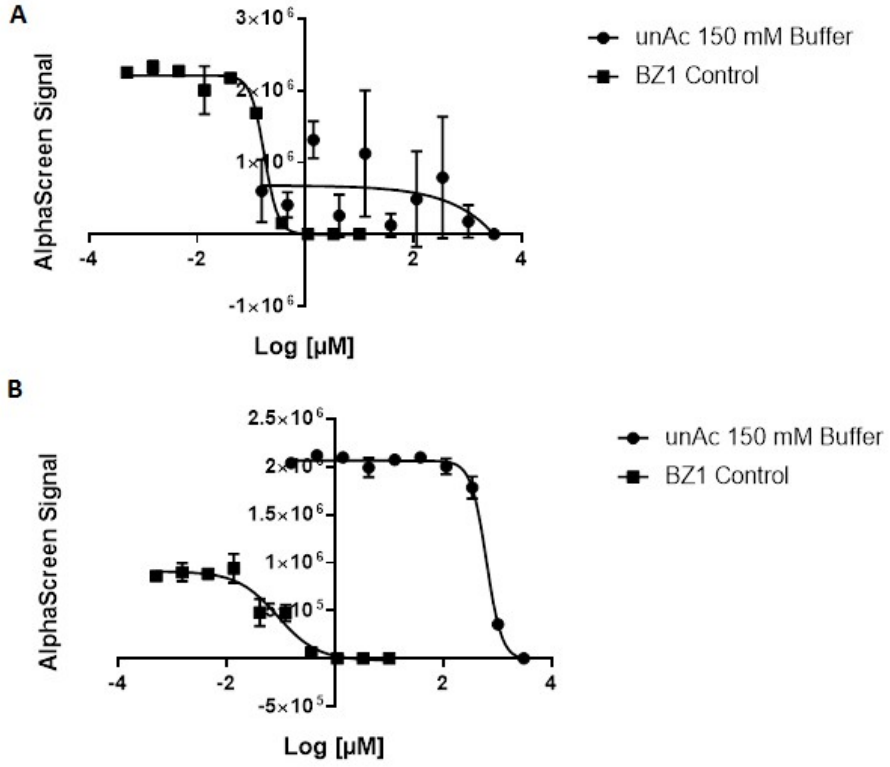

Figure 12: Negative Controls with BPTF and CECR2 using 150 mM Buffer. (A) Shown are the AlphaScreen dose-response curves for BPTF with H2A.Z I unAc and the control BZ1 using a 150 mM buffer. **(B)** Shown are the dose-response curves for CECR2 with H2A.Z I unAc and the control BZ1 using a 150 mM buffer.

Acetyl-group Mimic Experiments

As previously stated, the synthesized peptides were purified as trifluoroacetate salts. Each diacetylated peptide has a charge of +5 at the buffer pH of 7.4 meaning that the trifluoroacetate concentration in the peptide stocks could potentially be up to five times the concentration of the

peptide. Along with potentially impacting the pH, it is possible that the trifluoroacetyl group acts as an acetyl group mimic with affinity for the bromodomain acetyl lysine binding pocket (Figure 13). This would account for the unexpectedly low IC_{50} values obtained for BPTF and the diacetylated peptides without an observed decrease in the maximum signal intensity. This would also account for the observed binding of the nonbinding negative control peptides. Therefore, two AlphaScreen competition experiments were performed using sodium trifluoroacetate to determine if it can competitively bind the BPTF and CECR2 bromodomains. The results are shown in Figures 14 and 15 for BPTF and CECR2, respectively. While the IC_{50} values could not be calculated from either assay as neither reached 50% signal inhibition, it is apparent that sodium trifluoroacetate produces an inhibitory effect in both cases. There is a significant decrease in signal seen in the BPTF assay at higher concentrations reaching almost 50% and a milder, yet still notable, signal decrease of about 25% for CECR2. This suggests that a higher trifluoroacetate concentration range may reveal competitive binding with the BPTF and CECR2 bromodomains. The reported AlphaScreen IC_{50} values for several bromodomains with other acetyl group mimics are well into the mM range[56] further supporting this idea. Therefore, a follow up experiment using a higher NaTFA concentration range could be performed to test this idea.

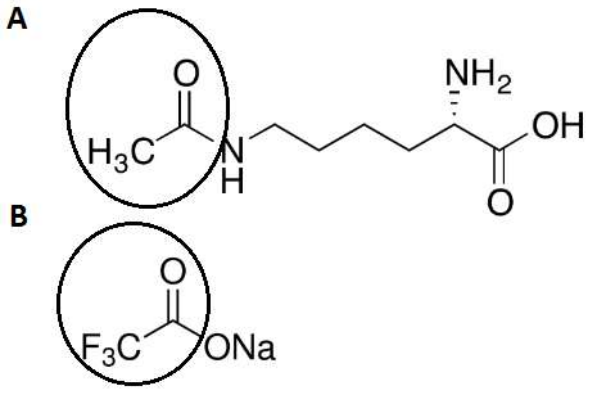

Figure 13: Acetyl-group Mimic (A) Shown is N-ε-acetyl-l-lysine and (**B)** sodium trifluoroacetate. Circled is the acetyl group on lysine and the potential acetyl group mimic on sodium trifluoroacetate.

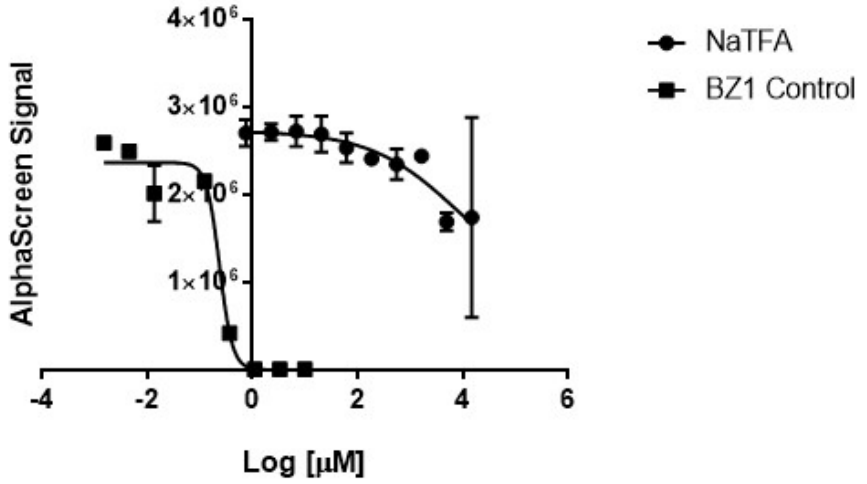

Figure 14: BPTF with NaTFA Dose-Response Curve. Dose-response curves for BPTF with sodium trifluoroacetate (NaTFA) and the BZ1 control. $R^2 = 0.57$ for the NaTFA curve ($IC_{50} = 0.24$ μM for BZ1 control and $R^2 = 0.98$ for BZ1 control).

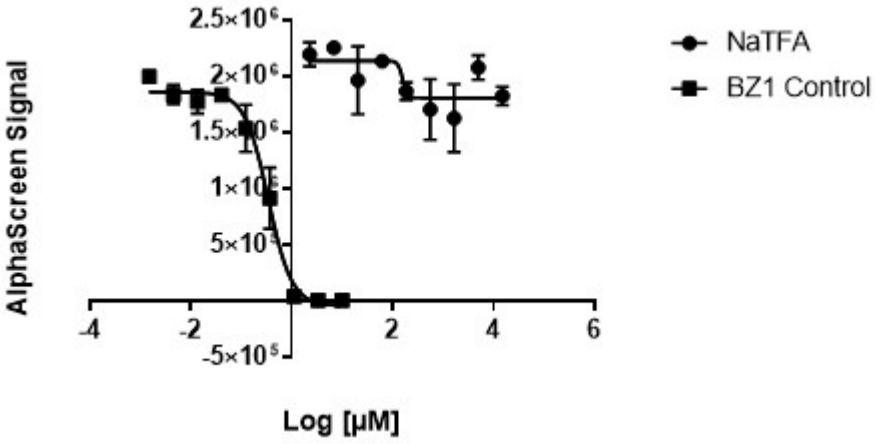

Figure 15: CECR2 with NaTFA Dose-Response Curve. Dose-response curves for CECR2 with sodium trifluoroacetate (NaTFA) and the BZ1 control. $R^2 = 0.42$ for the NaTFA curve ($IC_{50} = 0.34$ μM for BZ1 control and $R^2 = 0.98$ for BZ1 control).

Conclusion

The current project included two components: 1) the characterization of the CECR2 bromodomain binding interactions with diacetylated H2A.Z peptides and 2) the optimization of the AlphaScreen assay for the CECR2 bromodomain and H2A.Z peptides to evaluate the assay's potential for characterizing these types of interactions. Originally, the intention was to determine CECR2's preferred binding motif through the characterization of its binding interactions with all of the H2A.Z I and II diacetylation patterns using the AlphaScreen assay. However, as the optimization process turned out to be more complex than expected this was not possible. Instead, a handful of the H2A.Z I diacetylated peptides were used with the assay, and while IC_{50} values for CECR2 were obtained, their accuracy remains unclear.

The optimization of the assay for BRD-peptide binding interactions began by attempting to validate the assay using literature PrOF NMR K_d values for BPTF and diacetylated H2A.Z I peptides. Unfortunately, the obtained AlphaScreen IC_{50} values were much lower than expected and could not be rank ordered with the BPTF PrOF NMR K_d's. This led to the idea that the assay may have a limited dynamic range for resolving different affinities leading to an attempt at determining the dynamic range. This was done using peptides with previously reported binding affinities at one extreme end of the affinity range, mainly nonbinding and weak binding peptides (negative controls). Unfortunately, there was too much variation in the results to confidently draw any conclusions. However, the majority of IC_{50} values obtained using the negative controls were much lower than expected leading to the investigation of a potential assay artifact. As the peptides were purified as trifluoroacetate salts, and residual trifluoracetic acid was thought to affect the pH, the pH of the peptide solutions was first determined. They were found to be more acidic (pH ~ 5) than expected (pH ~ 7.4) leading to the determination as to whether pH has an effect on the IC_{50}. It was found that the IC_{50} decreases with decreasing pH. However, when trying to correct for the problem of low pH by using a buffer with increased buffer capacity, there was no notable difference in the IC_{50} values obtained for assays in which higher and lower buffer

capacity solutions were used. This was the case despite the higher strength buffer's successful maintenance of the peptide solutions' pH at 7.4. Therefore, although lower pH does appear to result in lower IC_{50} values, the lower pH observed for the highest concentration peptide solutions does not appear to be solely responsible for the unexpectedly low IC_{50} values obtained for BPTF and the diacetylated peptides. One final factor was considered regarding the trifluoroacetate salts. Trifluoroacetate was investigated as a potential acetyl group mimic which could account for the unexpectedly low IC_{50} values obtained for BPTF with diacetylated peptides and the observed binding of the nonbinding negative control peptides. The results indicated that trifluoroacetate shows some inhibition activity for both BPTF and CECR2 posing a number of potential future experiments. Along with the follow up experiment suggested in the Results/Discussion section using a higher NaTFA concentration range, another experiment could be performed to determine whether the presence of NaTFA with a positive control such as BZ1 notably affects the IC_{50}. If this is found to be the case, an additional future experiment could be performed to evaluate the peptides as HCl salts verses TFA salts by performing a peptide counter-ion exchange.

The continued efforts to optimize the AlphaScreen assay for BRD-peptide binding interactions, especially the further investigation into the potential effects of trifluoroacetate salts, may prove promising. However, the sensitivity and variability demonstrated by the AlphaScreen assay to the assay conditions used for this research suggest that these types of interactions may be better characterized by PrOF NMR. The K_d of CECR2 with the H2A.Z I AcK 7, 13 peptide was determined here to be 115 μM which was in agreement with the literature PrOF NMR K_d reported to be 130 μM.[16] Future work would therefore include the characterization of CECR2 binding interactions with the diacetylated H2A.Z I and II peptides as was originally intended, but by PrOF NMR while continuing to optimize the AlphaScreen assay for these interactions beginning with the experiments suggested above.

Materials and Methods

Peptide Synthesis

Peptide Synthesis: All peptides were synthesized using *N*-9-fluorenylmethoxycarbonyl (Fmoc) solid phase synthesis methods on NovaSyn TGR resin (Novabiochem, 0.24 mmol/g) on a 0.025 mmol scale using 4 equivalent masses of each reagent relative to the resin. The synthesis was performed using a Liberty Blue automated microwave synthesizer. The amino acid coupling steps were accomplished using *N,N'*-diisopropylcarbodiimide (DIC) and Oxyma. The deprotection steps were performed using a 20% piperidine in N,N-dimethylformamide (DMF) solution.

Cleavage and Purification: Upon completion of the final coupling and Fmoc deprotection steps, all peptides were cleaved from the resin through the addition of a 92.5/2.5/2.5/2.5 trifluoroacetic acid (TFA)/triisopropylsilane (TIPS)/thioanisole/water cleavage cocktail which was allowed to stir for 2-5 hours. The cleavage reaction was followed by the evaporation of the solvent under a nitrogen stream. The crude peptides were then precipitated using chilled diethyl ether. Following centrifugation (4000 x g, 4°C, 5 min.) and decanting of the ether, the crude peptide mixture was dissolved in Milli-Q water and ultimately purified by reverse phase high-performance liquid chromatography (RP-HPLC) on a C-18 semi-prep peptide column. The peptides were eluted using a 0.1% TFA water and a 0% to 20% CH_3CN elution gradient over 25 minutes. The peptide molecular weight was verified using an Ab Sciex TOF/TOF 5800 matrix-assisted laser desorption ionization (MALDI) mass spectrometer using a 2,5-dihydroxybenzoic acid matrix. The final purity was verified via analytical RP-HPLC on a C-18 column using a 0.1% TFA water and a 0% to 50% CH_3CN elution gradient over 50 minutes. For each purified peptide, a quality control MALDI spectrum and HPLC chromatogram were collected. Table 8 lists all the synthesized peptides along with their quality control data. The purified peptide HPLC traces are provided in Figure 16.

Table 8: Peptide QC Data. Synthesized peptides and their theoretical and observed m/z ratios for the expected protonated peptide masses obtained via MALDI mass spectrometry of the purified products. All peptide masses were verified.

Peptide	Theoretical $[m+H]^+$	Observed $[m+H]^+$	Sequence
H2A.Z I unAc	1978.07	1979.50	H_2N-YAGGKAGKDSGKAKTKAVSR-C(O)NH_2 *
		1979.22	
H2A.Z I AcK 13	2020.10	2021.38	
		2021.30	
H2A.Z I AcK 4, 7	2062.13	2063.31	
H2A.Z I AcK 4,11	2062.13	2063.50	
H2A.Z I AcK 4, 13	2062.13	2063.40	
H2A.Z I AcK 4, 15	2062.13	2063.50	
		2063.18	
H2A.Z I AcK 7, 11	2062.13	2063.17	
H2A.Z I AcK 7, 13	2062.13	2063.93	
		2063.35	
H2A.Z I AcK 7, 15	2062.13	2064.00	
H2A.Z I AcK 11, 13	2062.13	2063.97	
H2A.Z I AcK 11, 15	2062.13	2063.39	
H2A.Z II AcK 7, 13	2032.12	2033.56	H_2N-YAGGKAGKacDSGKAKacAKAVSR-C(O)NH_2

*Each acetylated H2A.Z I peptide is acetylated on the lysine residue (s) corresponding to the AcK numbers listed in the table.

Figure 16: HPLC Traces of the Purified Peptides. Shown are the HPLC chromatograms of the purified peptides collected from the analytical RP-HPLC runs. Retention times were all between 7-10 minutes.

AlphaScreen

AlphaScreen Competition Assays with BPTF and CECR2: Peptide stock solutions with concentrations of 10-40 mM were prepared in Milli-Q water from the lyophilized purified peptides. The concentrations were determined via UV-Vis. spectroscopy using the extinction coefficient (ε) of tyrosine at 276 nm of 1450 $cm^{-1}M^{-1}$. A 50 mM HEPES Na buffer was prepared to 50 mM HEPES Na (ChemImpex), 100 mM NaCl (SigmaAldrich), 0.05% CHAPS (RPI) and

0.1% BSA (SigmaAldrich) with the pH adjusted to 7.4 using a calibrated pH electrode. The following reagents were used as listed in Table 9.

Table 9: AlphaScreen Reagents

Reagent	Stock Conc.	Info.
BZ1 inhibitor	4 mM	used in each experiment as a positive control
biotinylated H4 AcK 5, 8, 12, 16 peptide probe	25,000 nM	EpiCypher: Ac-SGRGKacGGKacGLGKacGGAKacRHRKVLR-Peg (Biot)
His_9-BPTF	15,000-20,000 nM	[] determined via UV-Vis. spectroscopy; $\varepsilon_{280\ nm}$ His_9-BPTF = 18910 $cm^{-1}M^{-1}$
His_9-CECR2	66,000 nM	EpiCypher
nickel chelate (Ni-NTA) acceptor beads	5000 µg/mL	Cat. #: 6760619M, AlphaScreen Histidine (Nickel Chelate) Detection Kit
streptavidin donor beads	5000 µg/mL	Cat. #: 6760619M, AlphaScreen Histidine (Nickel Chelate) Detection Kit

For each competition assay, three solutions were prepared at four times their final concentrations (see final concentrations in 1 and 2 below). These solutions are the biotinylated H4 peptide probe diluted in buffer, the protein stock solution diluted in buffer, and the highest concentration serial dilution solution containing protein stock solution and inhibitor/peptide stock solution diluted in buffer. Ten three-fold serial dilutions were prepared from the latter solution and the diluted protein stock solution keeping the protein concentration fixed while varying the inhibitor/peptide concentration. 5 µl of each serial dilution solution was then added to a 384-well plate (ProxiPlate-384, PerkinElmer) two times for one technical replicate each. This was followed by the addition of 5 µl of the diluted biotinylated H4 peptide probe solution. The nickel chelate acceptor beads and the streptavidin donor beads were then combined in buffer under low light conditions, and 10 µl of the solution was added to each well. The final reagent concentrations in each well were as follows:

1) BPTF: 50 nM biotinylated H4 peptide probe, 30 nM His_9-BPTF, 20 µg/mL acceptor beads, and 20 µg/mL donor beads.
2) CECR2: 100 nM biotinylated H4 peptide probe, 60 nM His_9-CECR2, 20 µg/mL acceptor beads, and 20 µg/mL donor beads.

Final peptide concentrations for the most concentrated serial dilution solution ranged from 900 μM – 3000 μM.

The plate was then sealed and incubated in the dark for 30 minutes. After incubation, the plate was read using a Tecan Spark plate reader. Data was fit to a sigmoidal 4-parameter logistic curve using GraphPad Prism 5 from which the IC_{50} values were calculated. For each competition experiment, the small molecule, and BPTF and CECR2 bromodomain inhibitor, BZ1 was used as a positive control. The highest final assay concentration for BZ1 was 10 μM.

Note: For the BZ1 control assays DMSO was also added to achieve a final concentration of 0.25% in each well.

pH Experiments: Two pH experiments were performed with His_9-CECR2 and BZ1 varying the pH of the buffer. For the first experiment, four 50 mM HEPES Na buffer solutions were prepared as previously described except the pH of each was adjusted to either 7.4, 6.8, 5.5 or 4.0 using a calibrated pH electrode. The AlphaScreen competition assay was then performed. In the second experiment, three 50 mM HEPES Na buffer solutions were prepared with the pH adjusted over a narrower range to either 7.4, 7.2, or 7.0. Again, the AlphaScreen competition assays was performed.

Buffer capacity experiments: Four HEPES Na buffer solutions of varying strengths were prepared (25 mM, 50 mM, 100 mM and 150 mM), and the AlphaScreen competition assay performed using each buffer strength with His_9-BPTF and the H2A.Z I AcK 7, 13 peptide. Additional competition assays were performed using the 150 mM HEPES Na buffer strength with the H2A.Z I unAc peptide and His_9-BPTF and His_9-CECR2.

Acetyl-group mimic experiments: A 1 M sodium trifluoroacetate solution was prepared and used in two AlphaScreen competition experiments with His_9-BPTF and His_9-CECR2. The highest final assay concentration of the sodium trifluoroacetate was 15 mM from which three-fold serial dilutions were prepared. BZ1 was used as a control.

Protein Expression

Transformation: Cells from the E.coli strain BL21 (DE3)* were transformed with the CECR2_pET-28a(+)-TEV plasmid (GeneScript, kanamycin resistance, His_9Tev tag). 1 µl of the plasmid was transferred to a 100 µl aliquot of cells and heat shocked on a heat block at 42˚C for 45 seconds. 900 µl of autoclaved Luria broth (LB) media was added and the cells allowed to grow in a shaker incubator at 250 rpm, 37°C for 90 minutes. 100 µL of transformed cell culture was then plated on a Luria agar + kanamycin plate. The plate was then placed in a 37˚C incubator and allowed to grow for 24 hours. The next day, the plate was parafilmed and stored at 4°C.

Protein expression: Five 5 mL aliquots of autoclaved LB media were pipetted into five snap cap culture tubes followed by 5 µL of 1000x kanamycin stock into each tube. Each tube was then inoculated with a colony from a plate grown with cells previously transformed with the CECR2_pET-28a(+)-TEV plasmid. The five snap culture tubes were then placed on the shaker incubator at 250 rpm, 37°C for 24 hours.

After 24 hours, the media in the snap culture tubes appeared cloudy indicating cell growth. All five tubes were then added to 1 L of autoclaved LB media to which 1 mL of 1000x stock kanamycin was then also added. The flask was placed on the shaker incubator at 250 rpm, 37°C. The optical dispersion of the culture at 600 nm (OD600) was periodically checked using the UV-Vis. spectrophotometer with autoclaved LB media as the blank until an OD600 of 0.6-0.8 was reached. The temperature of the shaker incubator was then reduced to 20°C for 30 minutes.

Defined media for ^{19}F tryptophan labelling was then prepared per the recipe listed in Table 10A. The media was autoclaved and 50 mL of glucose, 1 mL of $FeCl_3$, and 10 mL of Solution B (prepared per the recipe listed in Table 10B) were subsequently added. The pH was then adjusted to 7.2 using a calibrated pH electrode. Lastly, 4 mL of $MgSO_4$ was added to a final

volume of 1.015 L. Tryptophan was omitted from the media.

Table 10: Defined Media for ^{19}F Tryptophan Labelling. (A) Recipe for the first 950 mL of the defined media to which, after autoclaving, glucose, $FeCl_3$, and Solution B are added. (B) Recipe for 100 mL of Solution B which is filter sterilized prior to its addition to the media.

A

Ingredient	Amount Added to 950 mL H_2O (g)
alanine	0.50
arginine	0.40
asparagine	0.40
aspartic acid	0.40
cystine	0.05
glutamine	0.40
glutamic acid	0.65
glycine	0.55
histidine	0.10
isoleucine	0.23
leucine	0.23
lysine hydrochloride	0.42
methionine	0.25
phenylalanine	0.13
proline	0.10
serine	2.10
threonine	0.23
tyrosine	0.17
valine	0.23
adenine	0.50
guanosine	0.65
thymine	0.20
uracil	0.50
cytosine	0.20
sodium acetate	1.50
succinic acid	1.50
NH_4Cl	0.50
NaOH	0.85
K_2HPO_4	10.50

B

Ingredient	Amount Added to 100 mL H_2O (mg)
$CaCl_2$-$2H_2O$	20
$ZnSO_4$-$7H_2O$	20
$MnSO_4$-H_2O	20
thiamine	500
niacin	500
biotin	10

The cell culture was then centrifuged for 20 minutes at 6000 x g, 4°C. The pellet was resuspended in the defined media and 61 mg of 5-fluoroindole (60 mg/L) was added. The culture was placed back on the shaker incubator to recover for 1-2 hours at 250 rpm, 37°C. For the last 30-60 minutes of the recovery time, the culture was cooled to the induction temperature of 20°C.

Next, 0.238 g of solid isopropyl ß-D-1-thiogalactopyranoside (IPTG) was added to the culture inducing the bacteria to produce His_9-CECR2. Due to the defined media containing 5-fluoroindole in place of tryptophan, CECR2's tryptophan 457 is fluorinated. The culture was left to express 5FW-His_9-CECR2 in the shaker incubator for 24 hours at 250 rpm, 20°C.

After 24 hours, the culture was centrifuged at 8000 x g for 8 minutes at 4°C. The pellet was transferred to a 50 mL falcon tube using a small amount of media from the culture and centrifuged again at 8000 x g for 10 minutes at 4°C. The media was then decanted from the pellet and the pellet transferred to a 50 mL falcon tube and stored at -80°C until the protein was purified.

PrOF NMR

PrOF NMR: One PrOF NMR experiment was performed using 5FW-His_9-CECR2 and H2A.Z I AcK 7, 13. The experiment was performed on a Bruker Avance III HD 500 instrument which has a 5 mm Prodigy TCI inverse cryoprobe with a ^{19}F signal to noise ratio of 2000:1. The H2A.Z I AcK 7, 13 peptide stock solution was titrated into 500 µL aliquots of purified 53 µM 5FW-His_9-CECR2 protein diluted in buffer (50 mM Tris, 100 mM NaCl, pH 7.4) to which D_2O and 0.1% TFA were added to final concentrations of 5% D_2O and 0.05% TFA. Five solutions of equal volume were prepared with peptide concentrations of 0 mM, 0.2 mM, 0.4 mM, 0.8 mM and 1.6 mM. One-dimensional ^{19}F NMR spectra were then obtained for each titration at an O1P of -75 ppm, NS = 16, D1 = 1, and AQ = 0.5 (TFA reference set to -75.25 ppm) and an O1P of -125 ppm, NS = 750, D1 = 0.7, and AQ = 0.05 (protein resonances). The change in the chemical shift of the protein resonance ($\Delta\delta$) for each of the different peptide concentrations was plotted as a function of peptide concentration producing a binding isotherm (fit to equation 1) from which the dissociation constant (K_d) was calculated.

Bibliography

1. Noble D. (2015). Conrad Waddington and the origin of epigenetics. *The Journal of experimental biology*. **218**, 816–818.
2. Dupont C., Armant D.R., Brenner C.A. (2009). Epigenetics: definition, mechanisms and clinical perspective. *Seminars in reproductive medicine*. **27**, 351–357.
3. Waddington CH. (1956). Genetic assimilation of the bithorax phenotype. *Evolution*. ***10***, 1–13.
4. Berger SL, Kouzarides, T, Shiekhattar R, and Shilatifard A. (2009). An operational definition of epigenetics. *Genes & development*. **23**, 781–783.
5. Henikoff S, Smith MM. (2015). Histone variants and epigenetics. *Cold Spring Harb Perspect Biol*. **7**, a019364.
6. D'Urso A. and Brickner JH. (2014). Mechanisms of epigenetic memory. *Trends Genet.* **30**, 230-236.
7. Wu H and Sun YE. (2006). Epigenetic regulation of stem cell differentiation. *Pediatric research*. **59**, 21R–25R.
8. Esteller M. (2008). Epigenetics in evolution and disease. *Lancet*. **372**, S90-S96.
9. Zhang Y., Sun Z., Jia J., Du T., Zhang N., Tang Y., Fang Y., Fang D. (2021). Overview of histone modification. *Adv Exp Med Biol.* **1283**, 1-16.
10. Leeb M and Wutz A. (2012). Establishment of epigenetic patterns in development. *Chromosoma.* **121**, 251-262.
11. Chamberlain SJ and Lalande M. (2010). Angelman syndrome, a genomic imprinting disorder of the brain. *J. Neurosci*. **30**, 9958-9963.
12. Zoghbi HY and Beaudet AL. (2016). Epigenetics and Human Disease. *Cold Spring Harb Perspect Biol.* **8**, a019497.
13. Ganesan A, Arimondo PB, Rots MG, Jeronimo C and Berdasco M. (2019). The timeline of epigenetic drug discovery: from reality to dreams. *Clinical epigenetics*. **11**, 174.
14. Alberts B., Lewis J.A., et al. (2002). Chromosomal DNA and its packaging in the chromatin fiber. *Molecular Biology of the Cell 4th Edition*.
15. Cutter A.R., Hayes J.J. (2015). A brief review of nucleosome structure. *FEBS Lett.* **589**, 2914-2922.
16. Olson N.M., Kroc S., Johnson J.A., Zahid H., Ycas P.D., Chan A., Kimbrough J.R., Kalra P., Schönbrunn E., Pomerantz W.C.K. (2020). NMR analyses of acetylated H2A.Z isoforms identify differential binding interactions with the bromodomain of the NURF nucleosome remodeling complex. *Biochemistry*. **59**, 1871-1880.
17. Annunziato A.T. (2008). DNA packaging: nucleosomes and chromatin. *Nature Education* **1**, 26.
18. Kreienbaum C, Paasche LW, Hake SB. (2022). H2A.Z's 'social' network: functional partners of an enigmatic histone variant. *Trends Biochem Sci.* **20**, S0968-0004(22)00114-1.
19. Lewis TS, Sokolova V, Jung H, Ng H, Tan D. (2021). Structural basis of chromatin regulation by histone variant H2A.Z. *Nucleic Acids Res.* **49**, 11379-11391.
20. Lamaa A, Humbert J, Aguirrebengoa M, Cheng X, Nicolas E, Côté J, Trouche D. (2020). Integrated analysis of H2A.Z isoforms function reveals a complex interplay in gene regulation. *Elife*. **9**, e53375.
21. Colino-Sanguino Y, Clark SJ, Valdes-Mora F. (2022). The H2A.Z-nucleosome code in mammals: emerging functions. *Trends Genet.* **38**, 273-289.
22. Dunn CJ, Sarkar P, Bailey ER, Farris S, Zhao M, Ward JM, Dudek SM, Saha RN. (2017). Histone hypervariants H2A.Z.1 and H2A.Z.2 play independent and context-specific roles in neuronal activity-induced transcription of *Arc/Arg3.1* and other immediate early genes. *eNeuro*. **4**, ENEURO.0040-17.2017.
23. (2012). Vincent Allfrey's work on histone acetylation. *J Biol Chem*. **287**, 2270-2271.

24. Josling, G. A., Selvarajah, S. A., Petter, M., & Duffy, M. F. (2012). The role of bromodomain proteins in regulating gene expression. *Genes*. **3**, 320–343.
25. Fujisawa, T., Filippakopoulos, P. (2017). Functions of bromodomain-containing proteins and their roles in homeostasis and cancer. *Nature reviews. Molecular cell biology*. **18**, 246–262.
26. Ferri E, Petosa C, McKenna CE. (2016). Bromodomains: Structure, function and pharmacology of inhibition. *Biochemical pharmacology*. **106**, 1–18.
27. Zaware N, Zhou MM. (2019). Bromodomain biology and drug discovery. *Nat Struct Mol Biol.* **26**, 870-879.
28. Kim K, Punj V, Choi J, Heo K, Kim J-M, Laird PW, An W. (2013). Gene dysregulation by histone variant H2A.Z in bladder cancer. *Epigenet. Chromatin.* **6**, 34.
29. Perell GT, Mishra NK, Sudhamalla B, Ycas PD, Islam K, Pomerantz WCK. (2017). Specific Acetylation Patterns of H2A.Z Form Transient Interactions with the BPTF Bromodomain. *Biochemistry*. **56**, 4607-4615.
30. Hasan, N., Ahuja, N. (2019). The emerging roles of ATP-dependent chromatin remodeling complexes in pancreatic cancer. *Cancers*. **11**, 1859.
31. Banting GS, Barak O, Ames TM, Burnham AC, Kardel MD, Cooch NS, Davidson CE, Godbout R, McDermid HE, and Shiekhattar R. (2005). CECR2, a protein involved in neurulation, forms a novel chromatin remodeling complex with SNF2L. *Human molecular genetics*. **14**, 513–524.
32. Norton KA, Niri FH, Weatherill CB, Williams CE, Duong K, and McDermid HE. (2021). Implantation failure and embryo loss contribute to subfertility in female mice mutant for chromatin remodeler Cecr2. *Biology of reproduction*. **104**, 835–849.
33. Thompson PJ, Norton KA, Niri FH, Dawe CE, and McDermid HE. (2012). CECR2 is involved in spermatogenesis and forms a complex with SNF2H in the testis. *Journal of molecular biology*. **415**, 793–806.
34. Wu L, Zhao G, Xu S, Kuang J, Ming J, Wu G, Wang T, Wang B, Zhu P, Pei D, and Liu J. (2021). The nuclear factor CECR2 promotes somatic cell reprogramming by reorganizing the chromatin structure. *The Journal of biological chemistry*. **296**, 100022.
35. Lee SK, Park EJ, Lee HS, Lee YS, Kwon J. (2012). Genome-wide screen of human bromodomain-containing proteins identifies Cecr2 as a novel DNA damage response protein. *Mol Cells.* **34**, 85-91.
36. Zhang, M., Liu, Z. Z., Aoshima, K., Cai, W. L., Sun, H., Xu, T., Zhang, Y., An, Y., Chen, J. F., Chan, L. H., Aoshima, A., Lang, S. M., Tang, Z., Che, X., Li, Y., Rutter, S. J., Bossuyt, V., Chen, X., Morrow, J. S., Pusztai, L., Rimm, D. L., Yin, M., Yan, Q. (2022). CECR2 drives breast cancer metastasis by promoting NF-κB signaling and macrophage-mediated immune suppression. *Science translational medicine*. **14**, eabf5473.
37. Divakaran A, Kirberger SE and Pomerantz WC. (2019). SAR by (protein-observed) ^{19}F NMR. *Acc Chem Res*. **52**, 3407-3418.
38. Arntson KE and Pomerantz WC. (2016). Protein-observed fluorine NMR: a bioorthogonal approach for small molecule discovery. *Journal of medicinal chemistry*. **59**, 5158–5171.
39. Kleckner IR and Foster MP. (2011) An introduction to NMR-based approaches for measuring protein dynamics. *Biochim Biophys Acta.* **1814**, 942-68.
40. Singh MK and Singh A. (2021). Characterization of polymers and fibers (the textile institute book series); Chapter 14 - Nuclear magnetic resonance spectroscopy. Woodhead Publishing. 321-339.
41. Becker W, Bhattiprolu KC, Gubensäk N and Zangger K. (2018). Investigating protein ligand interactions by solution nuclear magnetic resonance spectroscopy. *Chemphyschem.* **19**, 895-906.

42. Urick AK, Calle LP, Espinosa JF, Hu H and Pomerantz WC. (2016). Protein-observed fluorine NMR Is a complementary ligand discovery method to ^{1}H CPMG ligand-observed NMR. *ACS Chem Biol*. **11**, 3154-3164.
43. Schuff N. (2017). In vivo NMR methods, overview of techniques. *Encyclopedia of Spectroscopy and Spectrometry*. **3**, 211-215.
44. Yasgar A, Jadhav A, Simeonov A, Coussens NP. (2016). AlphaScreen-Based Assays: Ultra-High-Throughput Screening for Small-Molecule Inhibitors of Challenging Enzymes and Protein-Protein Interactions. *Methods Mol Biol*. **1439**, 77-98.
45. Watson VG, Drake KM, Peng Y, Napper AD. (2013). Development of a high-throughput screening-compatible assay for the discovery of inhibitors of the AF4-AF9 interaction using AlphaScreen technology. *Assay Drug Dev Technol*. **11**, 253-268.
46. Wigle TJ, Herold JM, Senisterra GA, Vedadi M, Kireev DB, Arrowsmith CH, Frye SV and Janzen WP. (2010). Screening for inhibitors of low-affinity epigenetic peptide-protein interactions: an AlphaScreen-based assay for antagonists of methyl-lysine binding proteins. *Journal of biomolecular screening*. **15**, 62–71.
47. User's Guide to Alpha Assays Protein:Protein Interactions. (2011). PerkinElmer. https://www.blossombio.com/pdf/products/UG_Alphatech.pdf.
48. Eglen RM, Reisine T, Roby P, Rouleau N, Illy C, Bossé R and Bielefeld M. (2008). The use of AlphaScreen technology in HTS: current status. *Curr Chem Genomics*. **1**, 2-10.
49. Arkin MR, Glicksman MA, Fu H, Havel JJ and Du Y. (2012). Inhibition of Protein-Protein Interactions: Non-Cellular Assay Formats. In S. Markossian (Eds.) et. al. *Assay Guidance Manual*. Eli Lilly & Company and the National Center for Advancing Translational Sciences.
50. Ycas PD, Zahid H, Chan A, Olson NM, Johnson JA, Talluri SK, Schonbrunn E and Pomerantz WCK. (2020). New inhibitors for the BPTF bromodomain enabled by structural biology and biophysical assay development. *Org Biomol Chem*. **18**, 5174-5182.
51. Kleckner IR and Foster MP. (2011). An introduction to NMR-based approaches for measuring protein dynamics. *Biochim Biophys Acta*. **1814**, 942-68.
52. Olins DE and Olins AL. (2003). Chromatin history: our view from the bridge. *Nature reviews. Molecular cell biology*. **4**, 809–814.
53. Filippakopoulos P and Knapp S. (2014). Targeting bromodomains: epigenetic readers of lysine acetylation. *Nat Rev Drug Discov.* **13,** 337–356.
54. Cochran AG, Conery AR and Sims RJ 3rd. (2019). Bromodomains: a new target class for drug development. *Nat Rev Drug Discov*. **18**, 609–628.
55. Zahid H, Buchholz CR, Ciccone MF, Chan A, Nithianantham S, Shi K, Aihara H, Fischer M, Schönbrunn E, dos Santos CO, Landry JW, and Pomerantz WCK. (2021). New design rules for developing potent cell-active inhibitors of the nucleosome remodeling factor (NURF) via BPTF bromodomain inhibition. *J. Med. Chem.* **64**, 13902-13917.
56. Philpott M, Yang J, Tumber T, Fedorov O, Uttarkar S, Filippakopoulos P, Picaud S, Keates T, Felletar I, Ciulli A, Knapp S, and Heightman TD. (2011). Bromodomain-peptide displacement assays for interactome mapping and inhibitor discovery. *Molecular bioSystems*. **7**, 2899–2908.
57. Chung C. (2012). Small molecule bromodomain inhibitors: extending the druggable genome. Lawton G and Witty DR. *Progress in Medicinal Chemistry*. **51**, 1-55.